Supplement of Atmos. Chem. Phys., 26, 9181–9205, 2026
https://doi.org/10.5194/acp-26-9181-2026-supplement
© Author(s) 2026. CC BY 4.0 License.

Atmospheric Chemistry and Physics
Open Access

Supplement of

Linking in-canopy chemistry to above-canopy O_3, BVOCs, and NO_x gas fluxes in the Amazon rainforest

Flossie Brown et al.

Correspondence to: Flossie Brown (flossie.brown@env.ethz.ch) and Colette L. Heald (colette.heald@env.ethz.ch)

The copyright of individual parts of the supplement might differ from the article licence.

Supplementary

Model Inputs

Figs. S1 to S3

Supplementary model description

Biogenic emissions

Horizontal wind velocity

Chemistry

K parameter and vertical mixing above the canopy

Vertical transport solver

Figs. S4 to S10

Table S1 to S2

Model Evaluation

Figs. S11 to S18

Results

Figs. S18 to S26

Model Inputs and Set-up

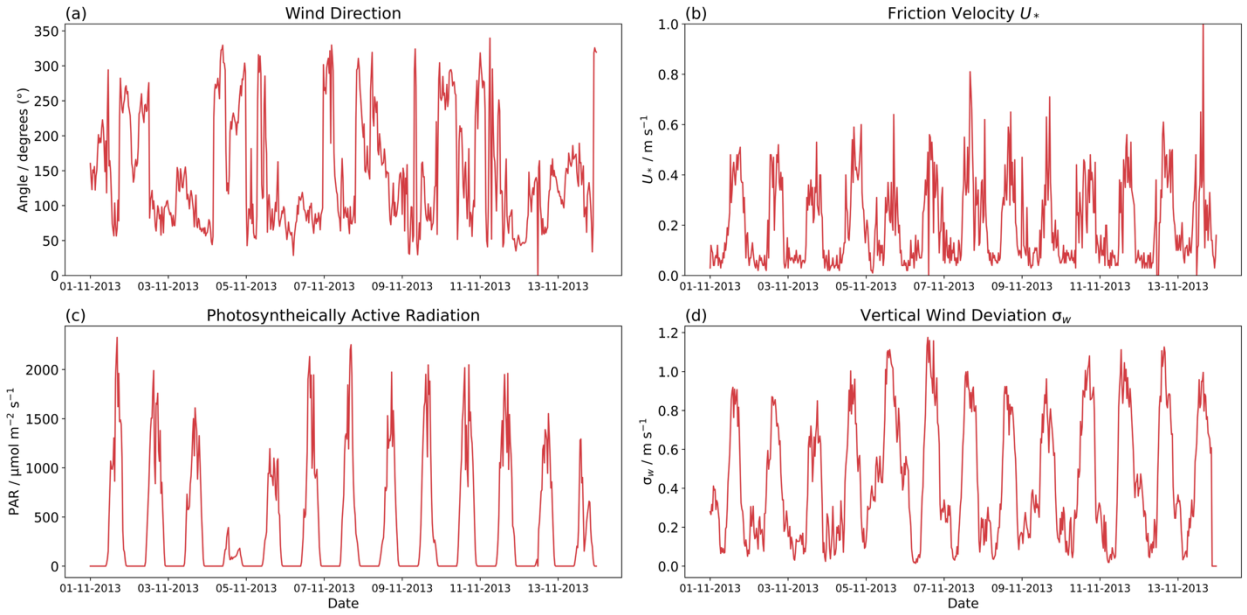

Figure S1: Driving data for simulations of November 2013, taken from observations at 55 m for (a) wind direction, (b) friction velocity (u_*), (c) photosynthetically active radiation (PAR). The vertical wind deviation (σ_w) in (d) is from November 2015.

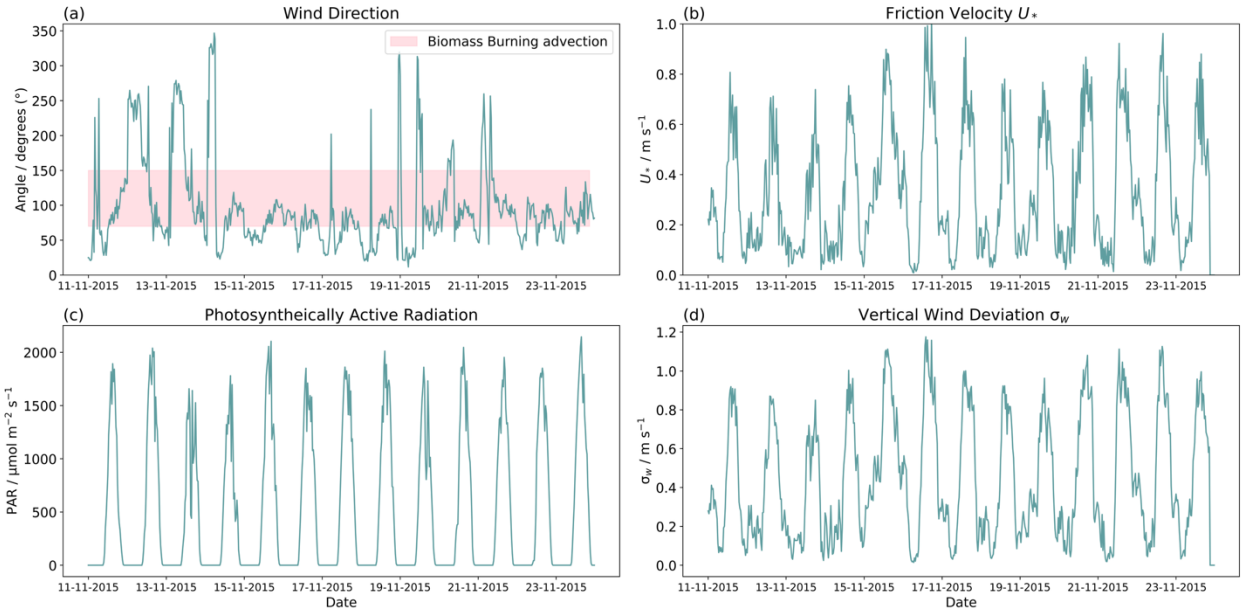

Figure S2: Driving data for simulations of November 2015, taken from observations at 55 m for (a) wind direction including the directions that biomass burning advection was triggered in the simulations (pink shading), (b) friction velocity (u_*), (c) photosynthetically active radiation (PAR) and (d) vertical wind deviation (σ_w).

Supplementary Model Description

Biogenic emissions

Emission factors from tropical forests and vertical mixing parameterizations remain highly uncertain and vary by location. We identify emission factors that best reproduce published observations and assess the sensitivity of canopy O_3 and NO_x exchange to these parameters. Table S1 summarises parameter values tested in 3-day sensitivity studies, with the final selection indicated (grey shading).

Sesquiterpene εp emission factor (nmol m^{-2} s^{-1})	**Monoterpene εs emission factor (nmol m^{-2} s^{-1})**	**Monoterpene εp emission factor (nmol m^{-2} s^{-1})**	**Soil NO emission factor (nmol m^{-2} s^{-1})**
0.08	DEFAULT: A-pin:0 D-lim:0	 A-pin:0.021 D-lim:0.017	0.0025
0	DEFAULT x2: A-pin:0 D-lim:0	 A-pin:0.042 D-lim:0.034	0.02
	LIGHT-DEPENDENT: A-pin:0.4 D-lim:0	 A-pin:0 D-lim:0.017	0.75

Table S1: Parameter values tested in biogenic emission sensitivity studies. Grey shading identifies the parameter that provides the best match to observations. Temperature sensitive emission factors are at 30°*C*.

The selected emission factors are somewhat lower than parameters suggested by Guenther et al. (2012) for a tropical evergreen forest. Calculations of εs for isoprene at the ATTO site by Gomes Alves et al. (2023) also found significant reductions from values suggested by Guenther et al. (2012) were required to reproduce observations. Furthermore, parameters suggested in Guenther

et al. (2012) include additional values which decrease the final emission flux including canopy reduction factors, leaf age factors and soil moisture and CO_2 parameters that are not included in this formulation. As a result, the emission factors here are not directly comparable.
In situ measurements of sesquiterpene concentrations at an Amazon site showed elevated sesquiterpene concentrations at night, in contrast to monoterpene emissions (see following), suggesting sesquiterpene emissions are temperature-dependent (Jardine et al. 2011). These measurements were taken in 2010 during the dry season at the TT34 flux tower. We use the approximate mean day and night vertical profiles recorded by Jardine et al. (2011, Fig. 3b) to identify an emission parameter that best reproduces these observations. The variability in sesquiterpene concentration with location and season is unknown, so the uncertainty in this emission factor is also unknown.

Figure S4 shows that the approximate concentration profile is reproduced above 10 m during the daytime and above 15 m during the nighttime. High concentrations observed close to the forest floor could be indicative of soil emissions of sesquiterpenes (e.g., Bourtsoukidis et al. 2018) but we exclude this from our preliminary study.

Monoterpenes have been recorded in the Amazon in an abundance of varieties. Whilst α-pinene and limonene are the most abundant, they account for less than 75% of recorded species (Yanes-Serrano et al., 2018). For simplicity, we only include these species in the model.

Default settings of FORCAsT v2 include temperature-dependent only emissions of α-pinene and limonene with emission factors (εp) of 0.021 and 0.017, respectively. The daily mean emission using these values is low compared to observed emissions from other tropical locations (Fig. S5), so we also test a doubling of the emission factors. We find observed diurnal cycles of monoterpene concentration from October 2015 (Gomes-Alves et al., 2023) are not well represented; simulated concentrations build-up overnight due to continued night-time emission at high temperature (Fig. S6). Several studies (e.g., Jardine et al. 2018), have suggested that α-pinene, in addition to other monoterpenes, has a light dependence in tropical tree species. We therefore include a light dependent emission factor (εs) for α-pinene and find better representation of the diurnal concentrations (Fig. S6).

NO emission factors from tropical soils remain uncertain. We test emission factors of 0.01, 0.02 and 0.03 nmol m^{-2} s^{-1} which results in mean NO emission fluxes of 4, 9 and 12 μgN m^{-2} hr^{-1}

within the large range of observations in Amazonia (Lee et al., 2024). Studies in pristine, undisturbed forest include measured emissions of 7.5 μgN m^{-2} hr^{-1} by Bakwin et al. (1990) and diurnally varying measurements of 12 μgN m^{-2} hr^{-1} at night to 16 μgN m^{-2} hr^{-1} in the day by Rummel et al. (2002).

These emission factors create 1 m concentrations of NO_2 that vary from 2 ppbv to 6 ppbv and NO concentrations at night of 1 ppbv to 8 ppbv, as NO emission factor increases (Fig. S8). Daytime ground-level NO is low in all cases. Observations by Rummel et al. (2002) find consistent NO concentrations at the soil level of a few ppbv, with O_3 concentrations of around 3 – 5 ppbv, whereas other studes (Bakwin et al., 1990) report lower values of 500 pptv. Top of canopy concentrations in sensitivity studies vary from 100 pptv NO_2 at night with the lowest emission factor to 400 pptv. In the day, NO_2 concentrations are often below 100 pptv. NO concentrations show morning peaks of 10 pptv with the lowest emission factor up to 80 pptv with the highest, with daytime average between 10 – 30 pptv. Most above canopy observations record NO concentrations below 50 pptv in pristine tropical environments (Bakwin et al. 1990; Kuhn et al., 2010; Rummel et al., 2002) and Cordova et al. (2004) find NO_2 concentrations of 350 pptv at night and 100 pptv in the day. To capture the above canopy NO_x concentrations within the range of observations, while avoiding NO_x build up in the lowest model layers, we select an emission factor of 0.2 nmol m^{-2} s^{-1}.

Fig. S10 evaluates the effect of changes in monoterpene, sesquiterpene and NO emissions factors on O_3 canopy fluxes and shows that the net effects of changes BVOC emissions is negligible. However, the small net effect from removing sesquiterpenes is caused by a decrease in chemical loss of 8 nmol m^{-2} s^{-1} than is almost compensated by an increase in deposition flux. Increasing the NO emission factor in intervals of 0.01 nmol m^{-2} s^{-1} increases the O_3 canopy flux by 3%.

Horizontal wind speed profiles

The horizontal wind speed (U) profile is first calculated above the canopy from observed u* at the canopy height (h):

$$U = \frac{u_*}{\kappa} \times \ln\left(\frac{z-d}{z_0}\right) \text{ [Eq. S1]}$$

Where $d=\frac{2}{3}h$ and z_0 is the surface roughness length (3.0 in the day and 1.0 in the night). z_0 was modified to reproduce observed wind speeds.

Below the canopy, the wind speed profile is further modified from the calculated wind speed at the canopy height (U_h):

$$U = U_h \times e^{-\alpha\frac{(1-z)}{h}} \quad \text{[Eq. S2]}$$

Where α is a wind extinction coefficient (=3.0). Smoothing below the canopy is applied to transition between below and above canopy equations.

Chemistry

We include sesquiterpene chemistry for the first time in FORCAsT v2. The first-order reaction rates for initial oxidation are included in Table S2.

Reaction	**Reaction rate constant (cm molecule^{-1} s^{-1})**
ß-carophyllene + OH	2x10^{-10}
ß-carophyllene + O_3	1.2x10^{-14}
ß-carophyllene + NO_3	2.2x10^{-11}

Table S2: Reaction rate of sesquiterpenes with oxidants in FORCAsT v2.

K parameter and vertical mixing above the canopy

Vertical mixing is an important control on concentrations and micrometeorological gradients.

The boundary layer height z_i is as described in Wei et al., (2022) and is computed from surface heat fluxes.

The surface layer (K_{sfc}) is considered the lower 10% of the boundary layer:

$$K_{sfc} = \frac{\kappa u_* z}{\Phi(\frac{z}{L})} \text{ [Eq. S3]}$$

Up to the boundary layer (K_{zi}):

$$K_{zi} = \frac{a\kappa u_* z(1-\frac{z}{z_i})^2}{\Phi(\frac{z}{L})} \text{ [Eq. S4]}$$

Where a = 1.23 to ensure a continuous transition between surface and boundary.

Above the boundary layer (K_{free}):

$$K_{free} = \kappa u_* \frac{z}{(1+\frac{\kappa z}{\lambda})^2} \text{ [Eq. S5]}$$

Where κ is the von Karman constant (0.41), z is the height above the ground (m), u_* is the friction velocity (m s^{-1}), λ is a function of the wind at the top of the boundary layer and the coriolis parameter, and $\Phi(\frac{z}{L})$ is a stability function (Wei et al., 2021; Nissanka et al., 2018). The stability function accounts for changing K in unstable, stable and neutral conditions. The derivation of the K equations are described by Nissanka et al. (2018) and evaluated in FORCAsT v2 by Wei et al. (2021).

K-theory is a simplification of true turbulence, not least because counter-gradient flow is known to occur (Oliveira et al., 2020). In addition, traditional K-theory does not account for 'near-field effects', which describes changes to conditions close to an emissions source or boundary, especially from a non-uniform source. Raupach et al. (1989) account for this near-field effect with an R factor, which is employed in the FORCAsT model:

$$R = \frac{1-e^{\frac{-\tau}{Tl}} \times (\tau - Tl)^{3/2}}{(\tau - Tl \times e^{\frac{-\tau}{Tl}})^{3/2}} \text{[Eq. S6]}$$

where *Tl* represents a Lagrangian timescale scaling factor (with u_* taken as the above-canopy value and fixed across heights). While the parameterisation of *Tl* in Eq. 1 is commonly used, alternative formulations have been proposed in the literature (e.g. Freire et al., 2017).

As described in the main text, the value τ/Tl is not constrained but is necessary for the calculation of the R factor (Eq. S6). Raupach et al. (1989) originally suggest τ/Tl = 1.1, while Wei et al. (2021) use τ/Tl = 4, which equates to a negligible reduction in K, reflecting the open canopy structure at the UMBS site.

We perform sensitivity studies to explore the effect of changing τ/Tl. The response of K is non-linear with changing τ/Tl; with τ/Tl =1.2 the mixing is strongly reduced and once τ/Tl =4, R is close to 1. The change in mixing between τ/Tl =1.6 and 4 does not result in significant changes in chemical profiles of O_3, isoprene, sesquiterpenes or NOx (Fig. S10). τ/Tl =1.2 is an extreme case as gas species accumulate to unreasonable concentrations within the canopy, and it should therefore be considered an unlikely scenario (Fig. S9). We choose τ/Tl =1.6 as it best represents the temperature profile and low concentrations of gas species in the lower canopy.

Evaluating the effect on O_3 canopy flux, a change in τ/Tl from 1.6 to 4 increases the total flux by 4% (Fig. S10), whereas reducing from 1.6 to 1.2 decreases the flux by over 9%. This suggests that low values of τ/Tl may be associated with higher uncertainty in canopy fluxes.

It should also be noted that changing the vertical profile of σ_w will produce different concentration profiles, so in that regard we have not fully explored the uncertainties in mixing. Although the UMBS site found no significant improvement when testing other expressions for $\sigma_{w(z)}$ within the canopy compared to a linear decrease, likely linked to the generally well-mixed conditions in the temperate forest (Wei et al., 2021), our simulations are sensitive to the changes in σ_w^2 with height, especially close to the surface. Observations in the literature (Santana et al., 2018; Freire et al., 2017) suggest mixing reduces rapidly within the Amazon rainforest canopy, such that the lower canopy is almost entirely separated from above. However, with only one in-canopy observation, it is not possible to conclusively determine the variation of σ_w at all model levels. Therefore, we highlight the necessity for measurements at more heights within the canopy.

Vertical transport solver

Equation S7 represents the continuous species continuity equation:

$$\frac{\partial c}{\partial t} = \frac{\partial}{\partial z}\left(\mathrm{K}\frac{\partial c}{\partial z}\right) + S_c + C \; [Eq.S7]$$

where c is the mixing ratio of a chemical species, S_c represents the sum of emissions, deposition, and advection tendencies at each layer (s^{-1}), C is net chemical production (s^{-1}), and K is the eddy diffusivity coefficient ($m^2\ s^{-1}$).

In the numerical implementation, the terms are operator split. Emissions, deposition, and advection tendencies are incorporated into the transport step (Eq. 13 in the main text), while gas-phase chemistry is solved subsequently in a separate chemistry step.

Source/sink tendencies (S_c) are represented in FORCAsT at each layer within the species continuity equation. Numerically, these tendencies are incorporated through operator splitting: S_c is multiplied by the model timestep Δt and added to the concentration field prior to solution of the implicit vertical diffusion equation, yielding $(I - \Delta t L)c^{n+1} = c^n + \Delta t S_c$, for timestep n

where L is the vertical transport operator. This means FORCAsT treats S_c as a concentration tendency, but integrates it separately from transport.

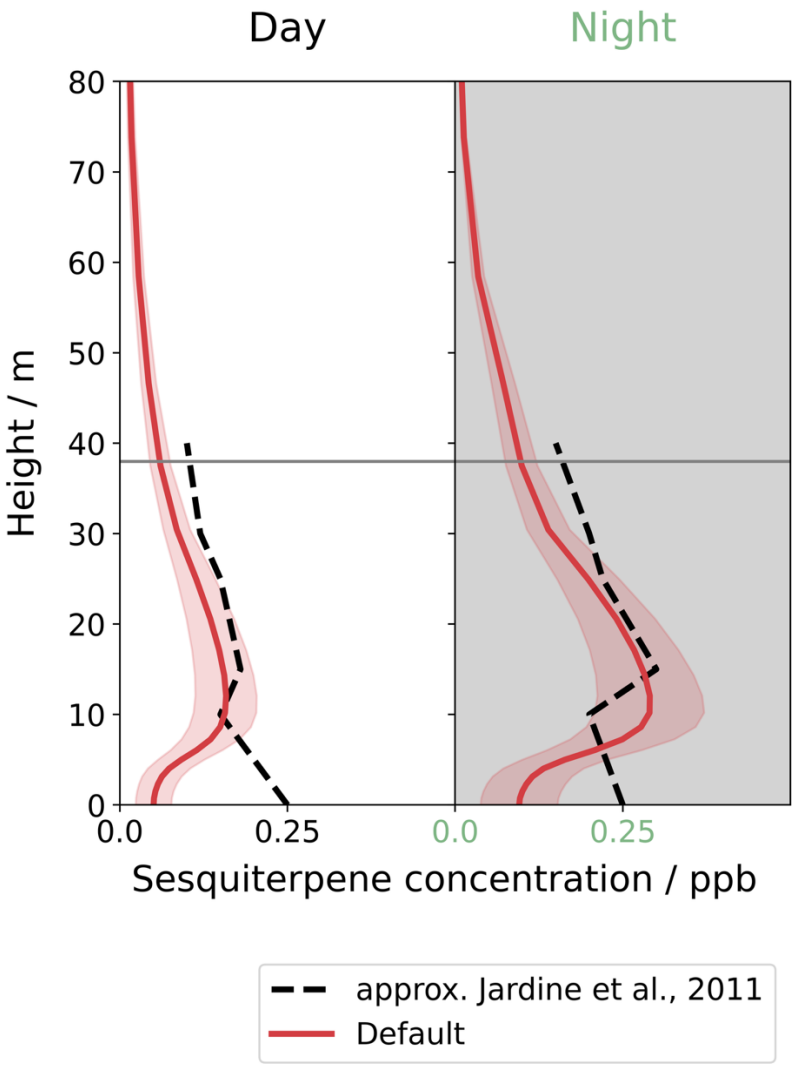

Figure S3: Vertical profile evaluation of sesquiterpene concentrations at different heights for day and night for simulations (red solid lines) and observations from Jardine et al. (2011) (black dashed line). The grey horizontal line indicates the canopy height. Shading indicates 1 standard deviation using daily means.

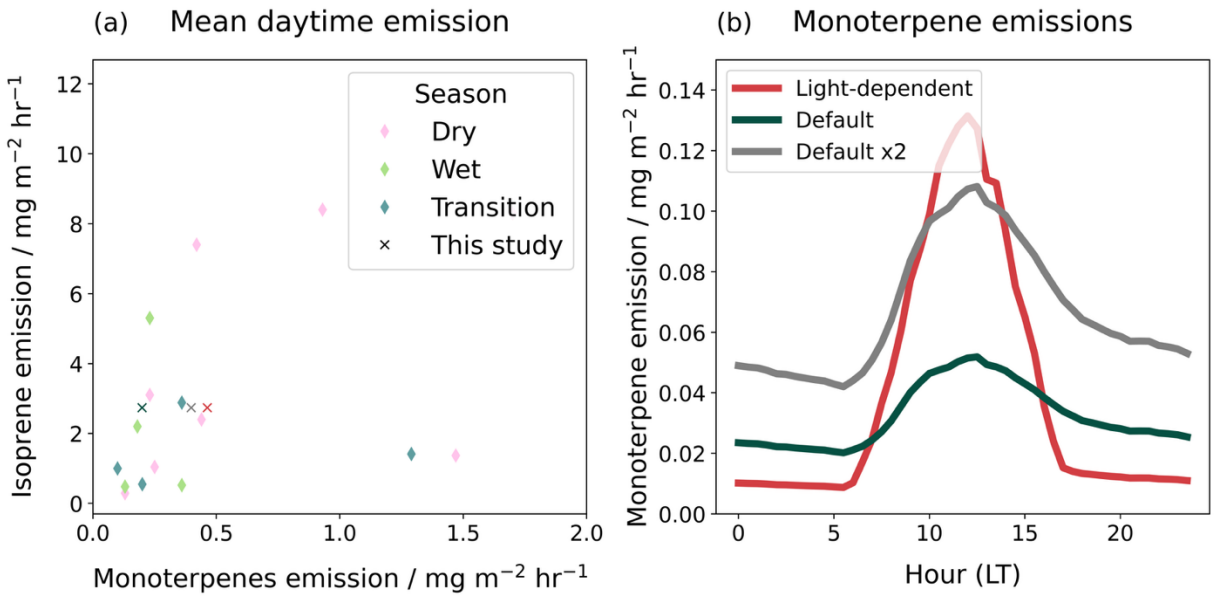

Figure S4: (a) Measured isoprene and monoterpene daytime (6:00 - 18:00) mean emission flux from studies of tropical species (Jardine et al., 2018) in comparison to emissions in this study (cross markers). (b) Diurnal mean emission rates of monoterpenes in the sensitivity tests in Table S1.

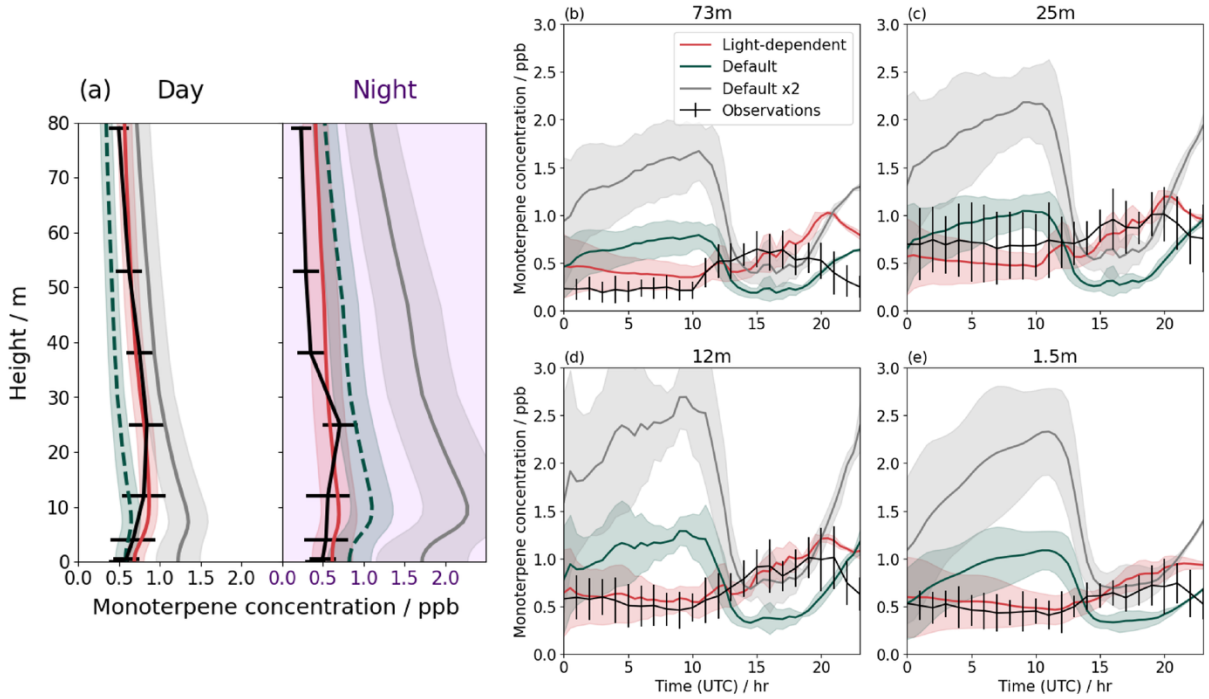

Figure S5: (a) Vertical profile evaluation at different heights and along the vertical profile for day and night. The grey horizontal line indicates the canopy height. Shading indicates 1 standard deviation using daily means. (b) – (e) Hourly mean total monoterpene evaluation compared to observations at 73 m, 25 m, 12 m and 1.5 m, respectively. Horizonal lines and shading show the daily mean standard deviation. Shading indicates 1 standard deviation from the 3-day simulation.

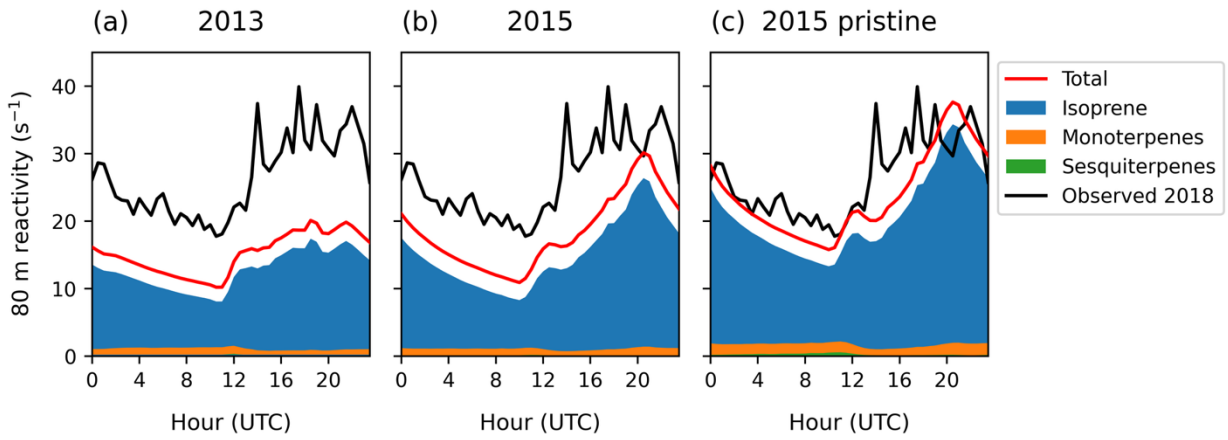

Figure S6: Total simulated OH reactivity at 80 m (red line) compared to observations in 2018 by Pfannerstill et al. (2018) (black solid line) for (a) 2013 simulation period, (b) the 2015 simulation period and (c) the 2015 simulation without transported NO_2. The simulated OH reactivity with respect to the primary emitted species are shaded.

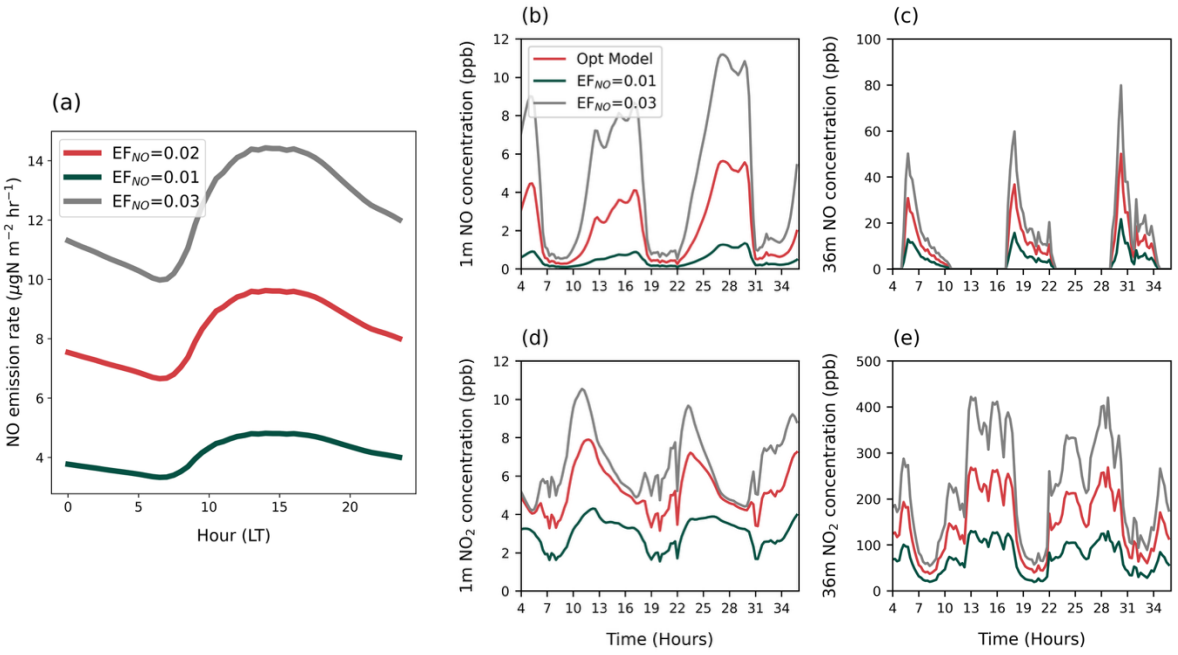

Figure S7: (a) Simulated diurnal mean emission rates of soil NO in the sensitivity tests, using 3 emission factors (nmol m^{-2} s^{-1}). (b) – (d) resulting NO and NO_2 concentrations from each sensitivity test. (b) NO concentration at 1m, (b) NO concentration at 36 m (canopy top), (c) NO_2 concentrations at 1 m (d) NO_2 concentration at 36 m (canopy top).

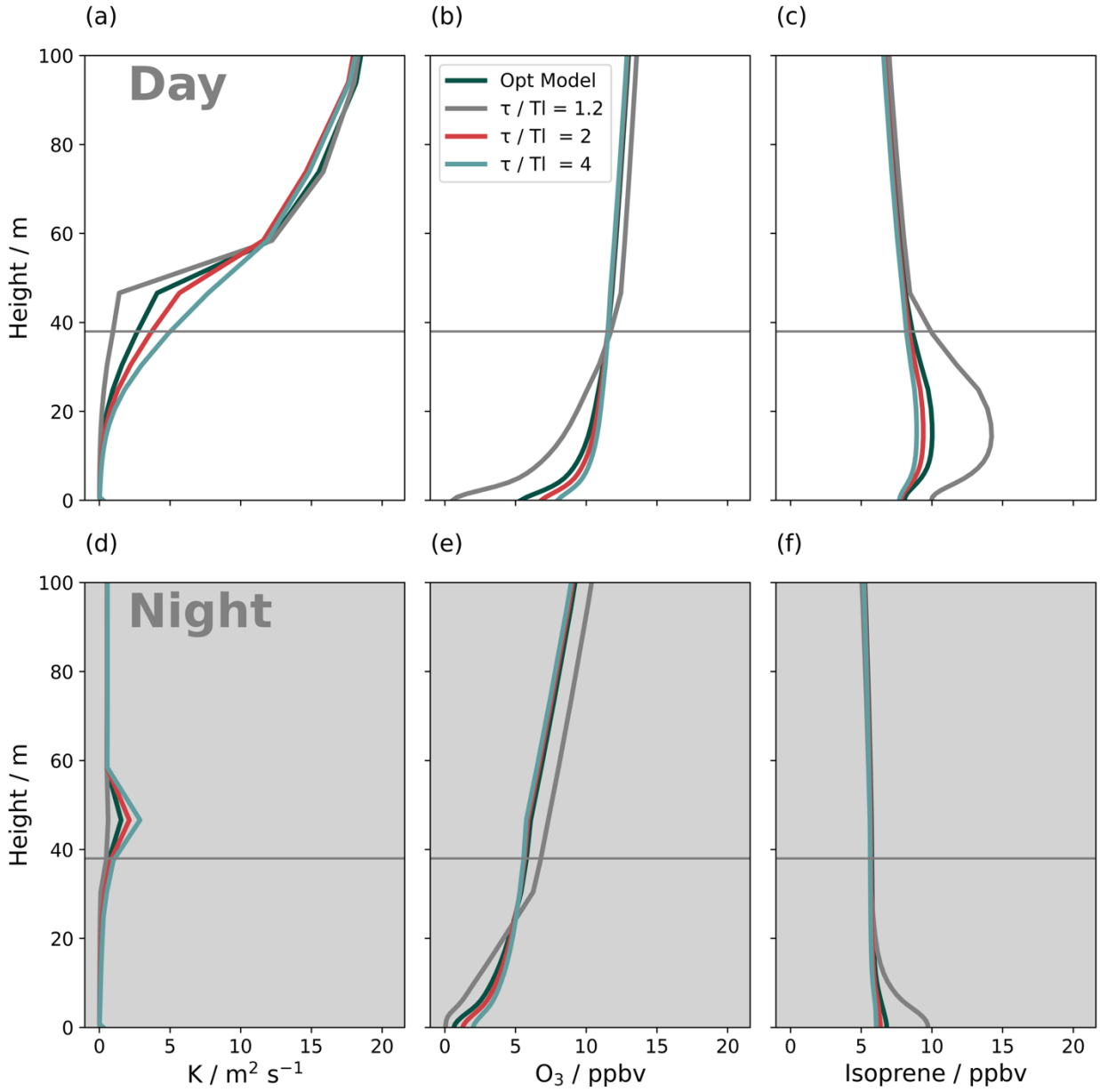

Figure S8: Daytime vertical mean profiles for (a) the eddy diffusivity parameter K with different values of τ/Tl and the resulting changes in trace gas profiles for (b) O_3, and (c) isoprene. The equivalent night time profiles are shown for (d) the eddy diffusivity parameter K, (e) O_3, and (f) isoprene. The optimum value is τ/Tl=1.6 (dark green line). The grey horizontal line indicates the canopy height.

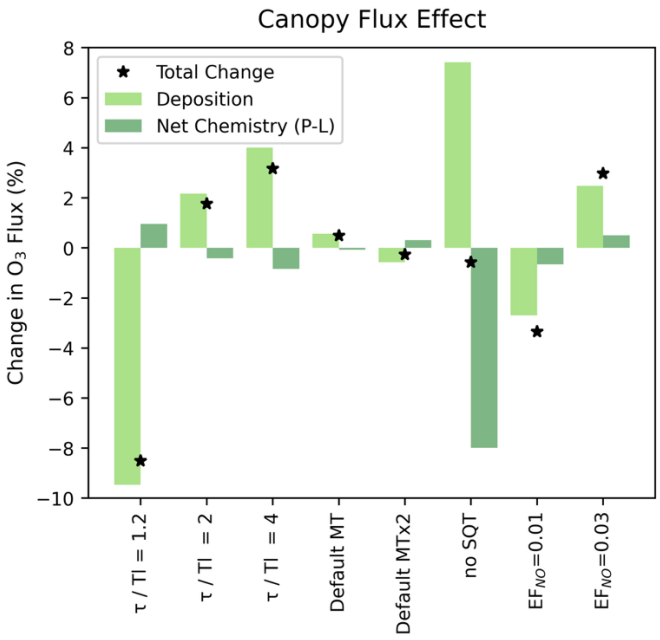

Figure S9: Percentage effect on total O_3 canopy flux (deposition and chemistry) compared to the final chosen parameters, and the net effect (black star). Negative values indicate lower O_3 loss in the canopy and positive values indicate more loss. Sensitivity tests are: 3 mixing parameters; 2 monoterpene emissions factors; without sesquiterpenes; 2 NO emission factors (Table S1).

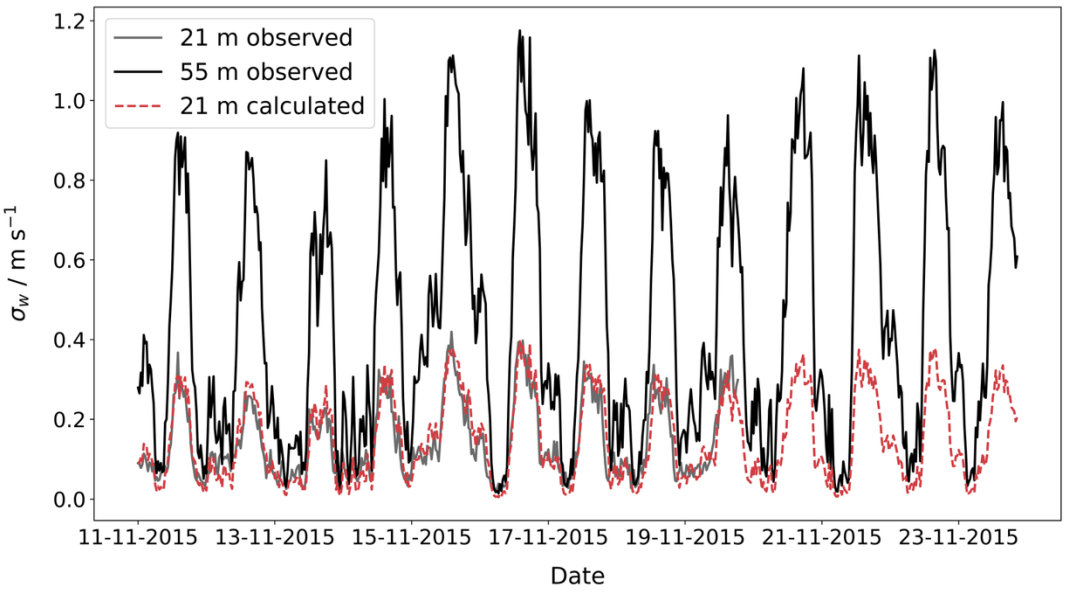

Figure S10: σ_w at 21 m calculated using Eq. 18 (red dashed line) from above canopy measurements at 55 m (black solid line). Calculated σ_w is close to observed values (grey solid line) at 21 m.

Model evaluation

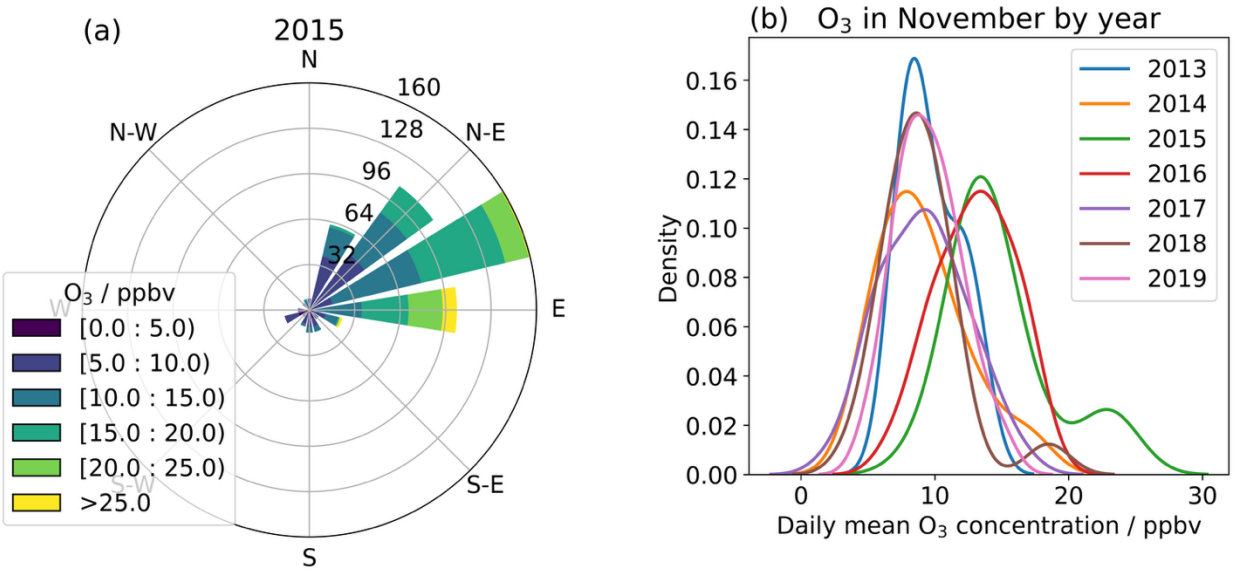

Figure S11: (a) Hourly O_3 concentrations organized by wind direction in November and (b) a density plot of daily mean O_3 concentrations in November measured at 36 m at ATTO for years 2013 – 2019 (https://www.attodata.org/).

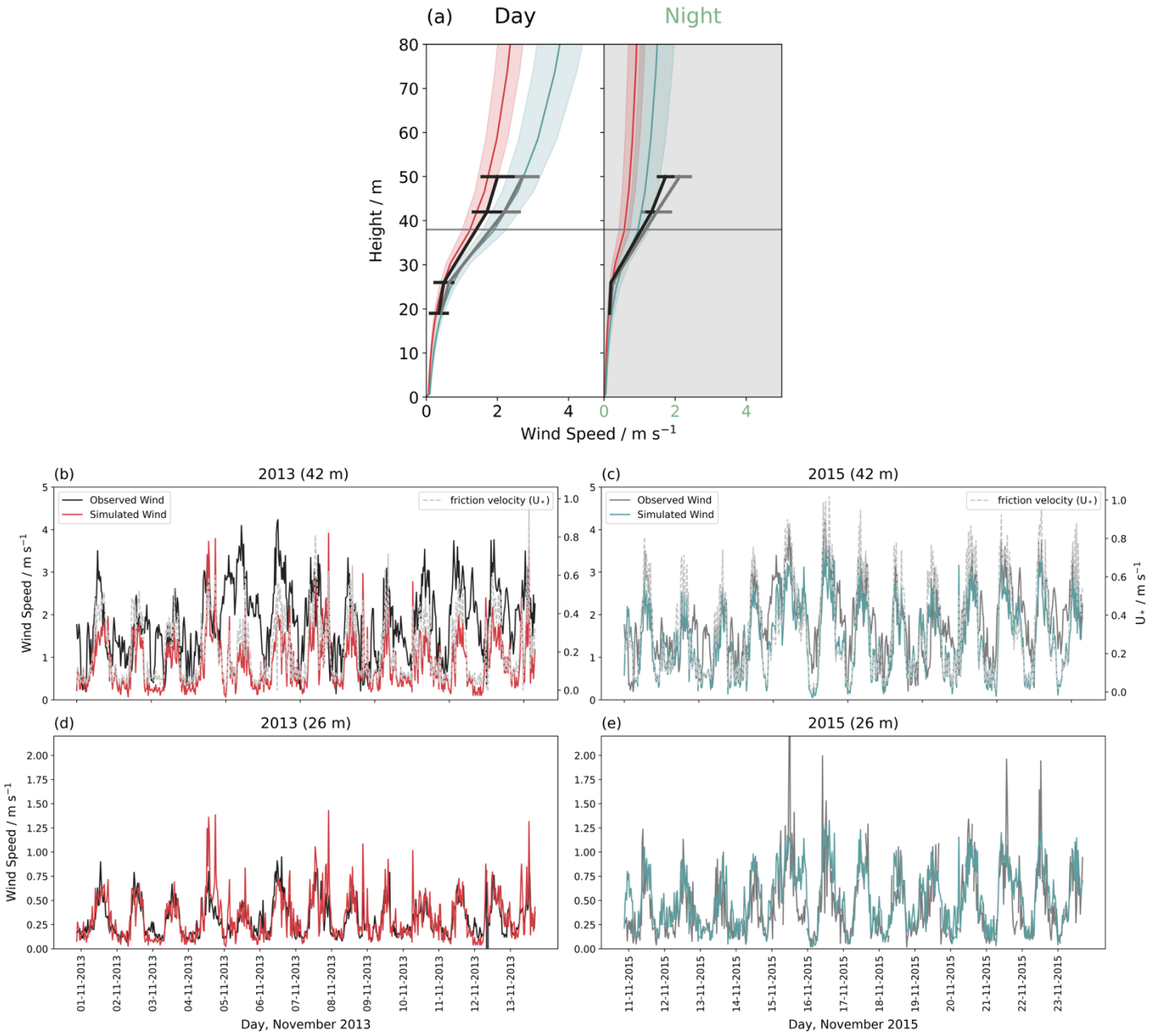

Figure S12: (a) Vertical profile evaluation of wind speed at different heights for day and night for simulations (coloured lines) and observations in 2013 (black solid line) and 2015 (grey solid line). Horizonal lines and shading show the daily mean standard deviation. (b) and (c) show the time series evaluation of horizontal wind speed and friction velocity at 42 m for the simulation period for (b) 2013 and (c) 2015. (d) and (e) show the time series evaluation of horizontal wind speed at 26 m for the simulation period for (d) 2013 and (e) 2015.

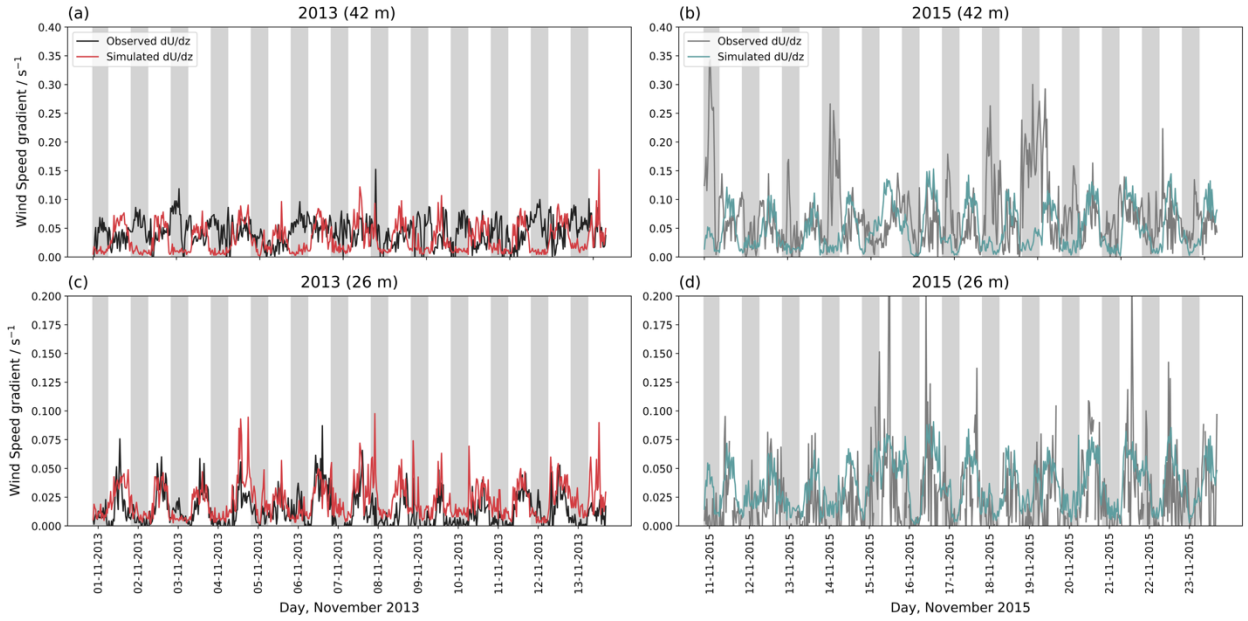

Figure S13: (a) and (b) Wind shear (dU/dz) at 42 m – 36 m for the (a) 2013 and (b) 2015 simulation periods. (c) and (d) Wind shear (dU/dz) at 26 m – 19 m for the (c) 2013 and (d) 2015 simulation periods.

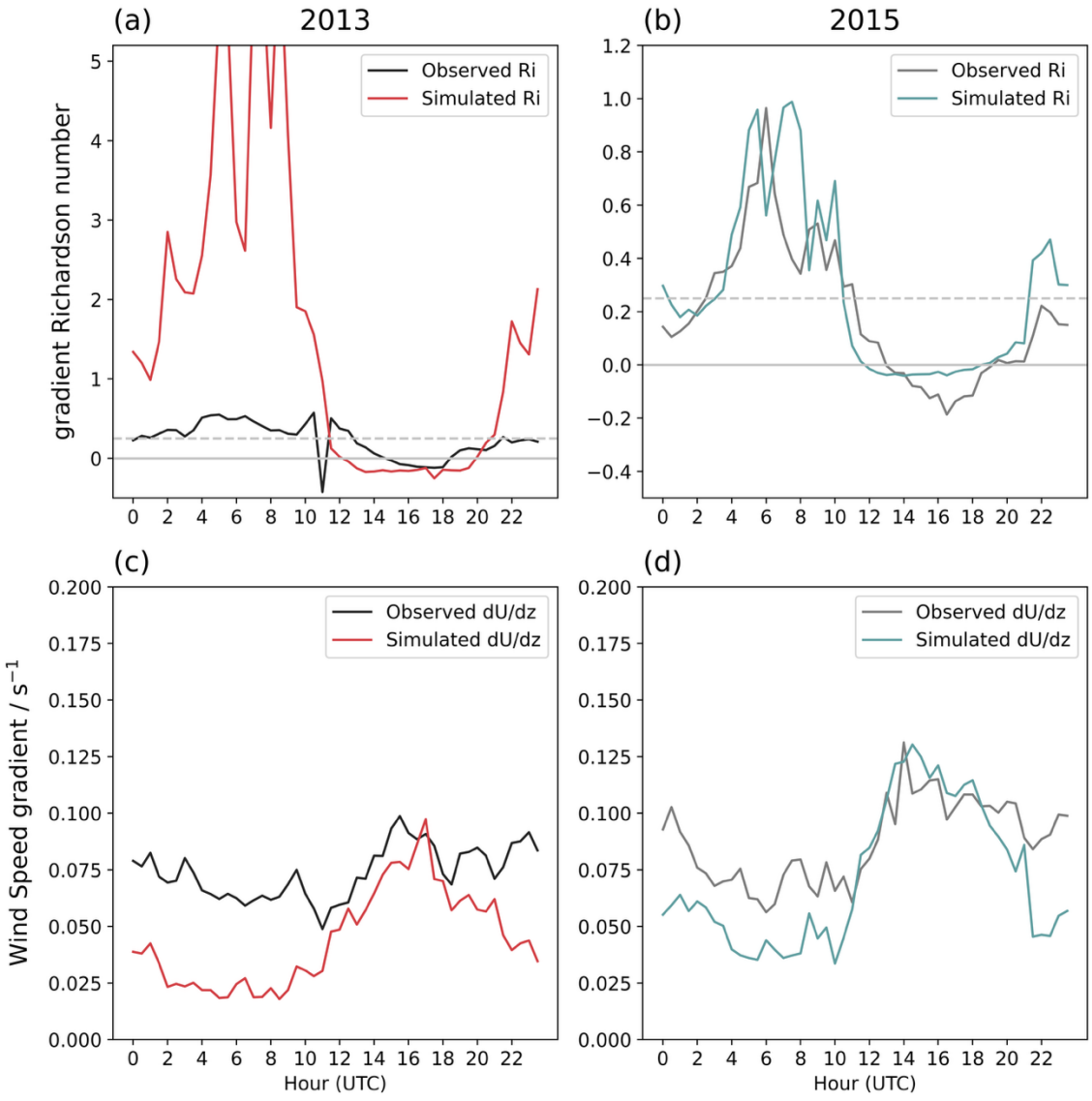

Figure S14: (a) and (b) Gradient Richardson number at 36 m for the (a) 2013 and (b) 2015 simulation periods. The boundary of highly turbulent (Ri < 0 , grey solid line) and stably stratified (Ri > 0.25, grey dashed line) are indicated with horizontal lines. (c) and (d) Wind shear (dU/dz) at 36 m for the (c) 2013 and (d) 2015 simulation periods.

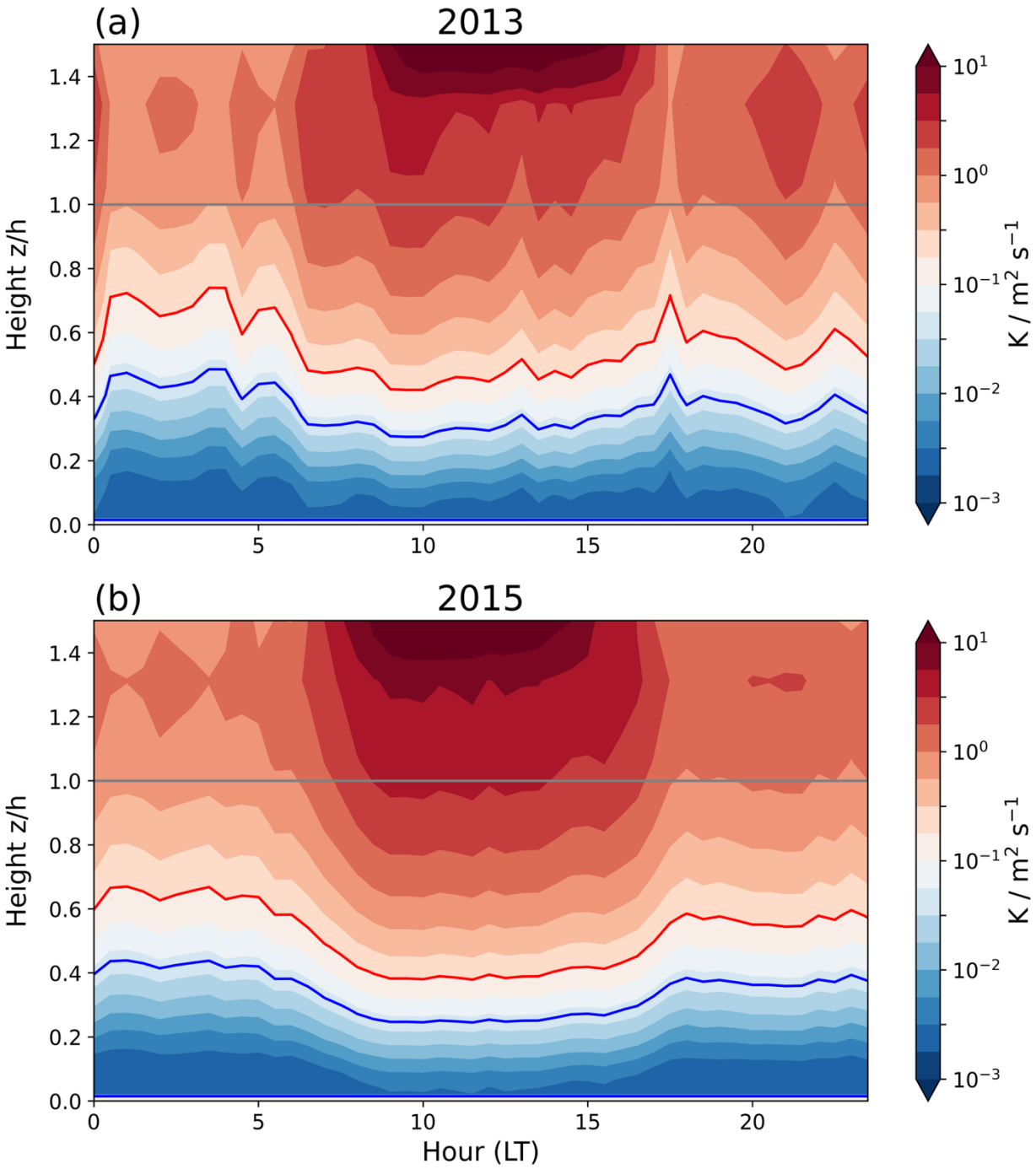

Figure S15: Diurnal mean eddy diffusivity parameter K over the simulation period in (a) 2013 and (b) 2015. The canopy height is indicated with a grey horizonal line. Red and Blue lines indicate well-mixed and poorly mixed limits suggested by Freire et al. (2017).

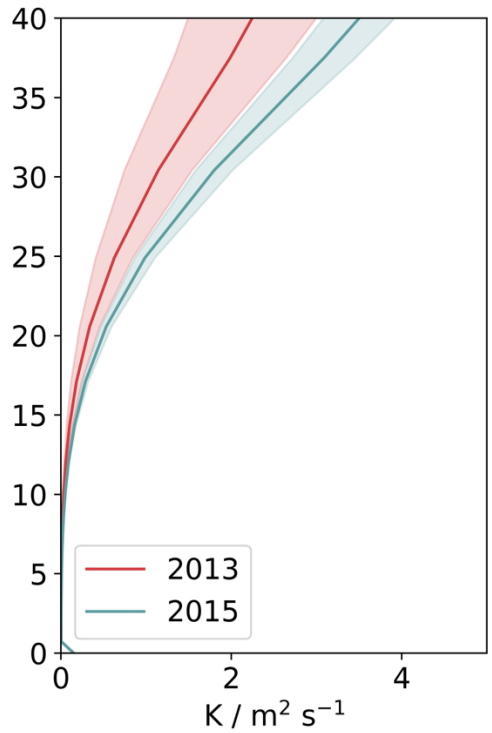

Figure S16: Daytime (06:00 – 18:00 LT) mean vertical profiles of simulated eddy diffusivity coefficient (K) from simulation periods in 2013 (red solid line) and 2015 (teal solid line), shading shows 1 standard deviation using daytime means.

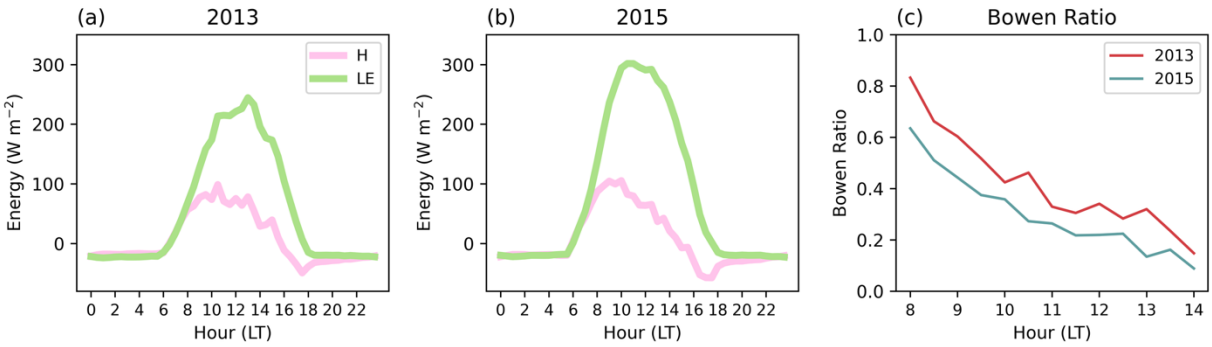

Figure S17: Half hourly mean latent heat (LE; green solid line) and sensible heat (H; pink solid line) fluxes from the canopy in (a) the 2013 simulation period and (b) the 2015 simulation period. (c) Half hourly mean Bowen ratio (LE/H) values for daytime (8:00 – 14:00 LT) for 2013 (red solid line) and 2015 (teal solid line).

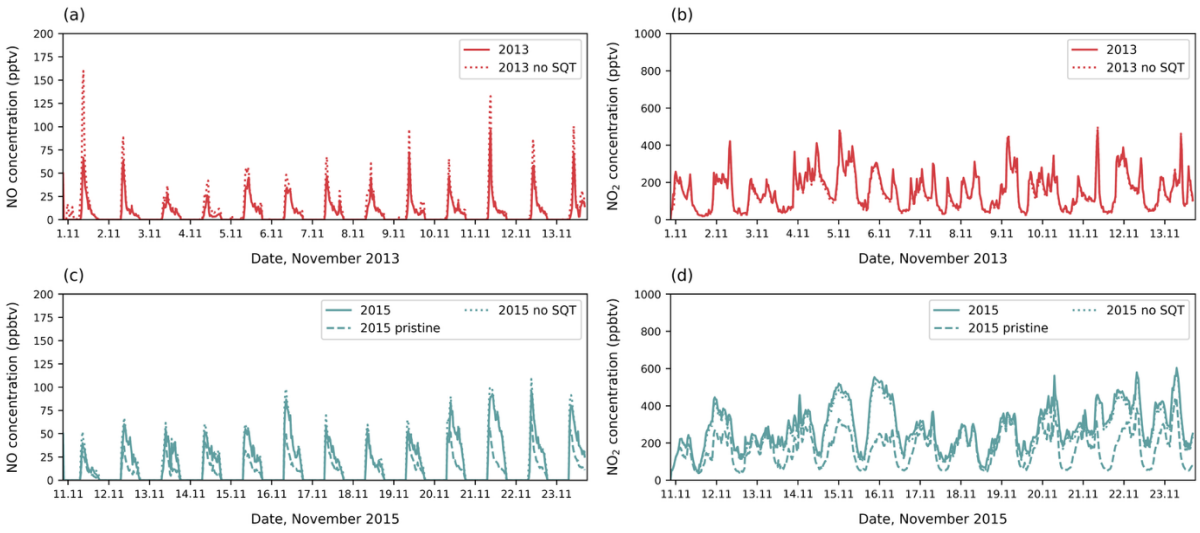

Figure S18: (a)– (d) Simulated NO and NO_2 at 36 m . (a) NO concentration in 2013, (b) NO_2 concentration in 2013 (c) NO concentrations in 2015 (d) NO_2 concentration in 2015.

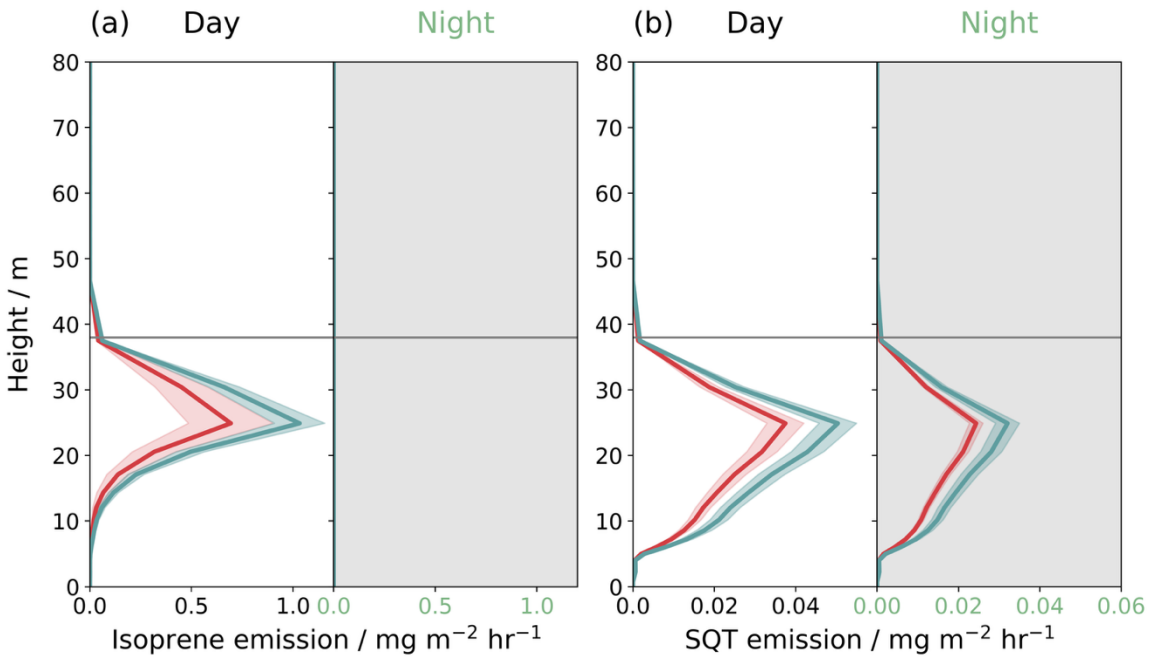

Fig. S19: Emission rates of (a) isoprene and (b) sesquiterpenes in 2015 (teal solid line) and 2013 (red solid line), presented as vertical profiles for day and night. Shading indicates 1 standard deviation using daily means.

Results

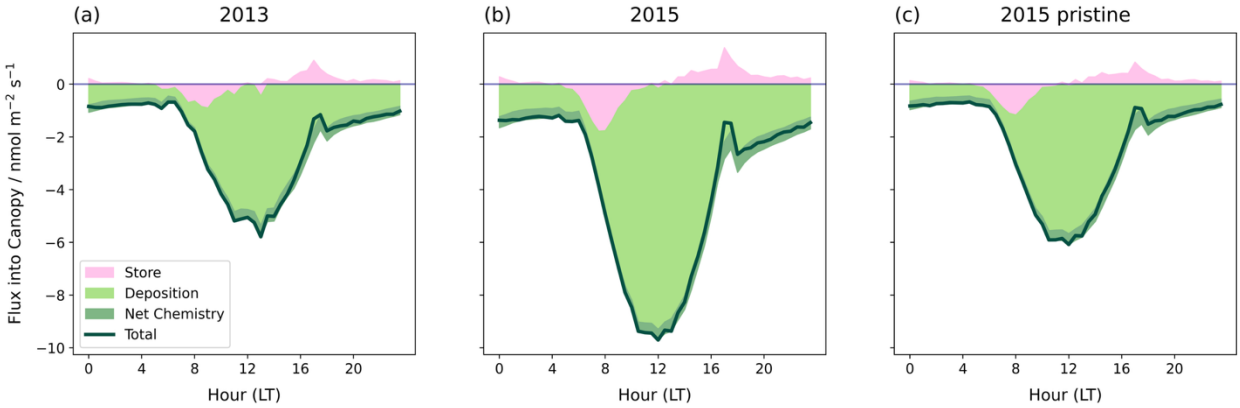

Figure S20: Mean O_3 diurnal cycle showing net chemistry (P-L) (dark green), deposition (light green) and storage within the canopy (pink) for (a) 2013, (b) 2015 including advection, (c) 2015 without advection. The sum of all terms (green solid line) is the total flux into the canopy.

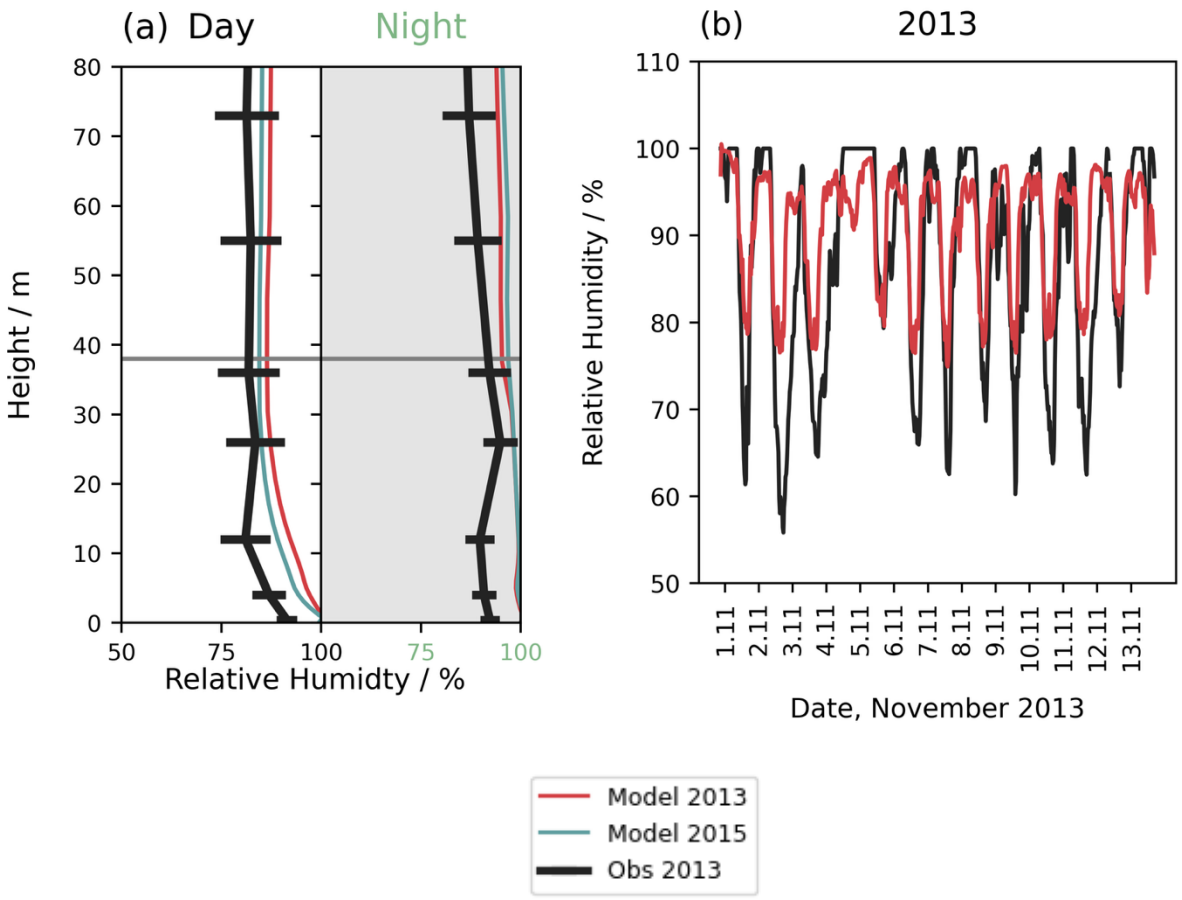

Figure S21: (a) Vertical profile evaluation of relative humidity at different heights for day and night for simulations (coloured lines) and observations in 2013 (black solid line). Horizonal lines show the daily mean standard deviation. (b) shows the time series evaluation of relative humidity at 36 m for the simulation period for 2013.

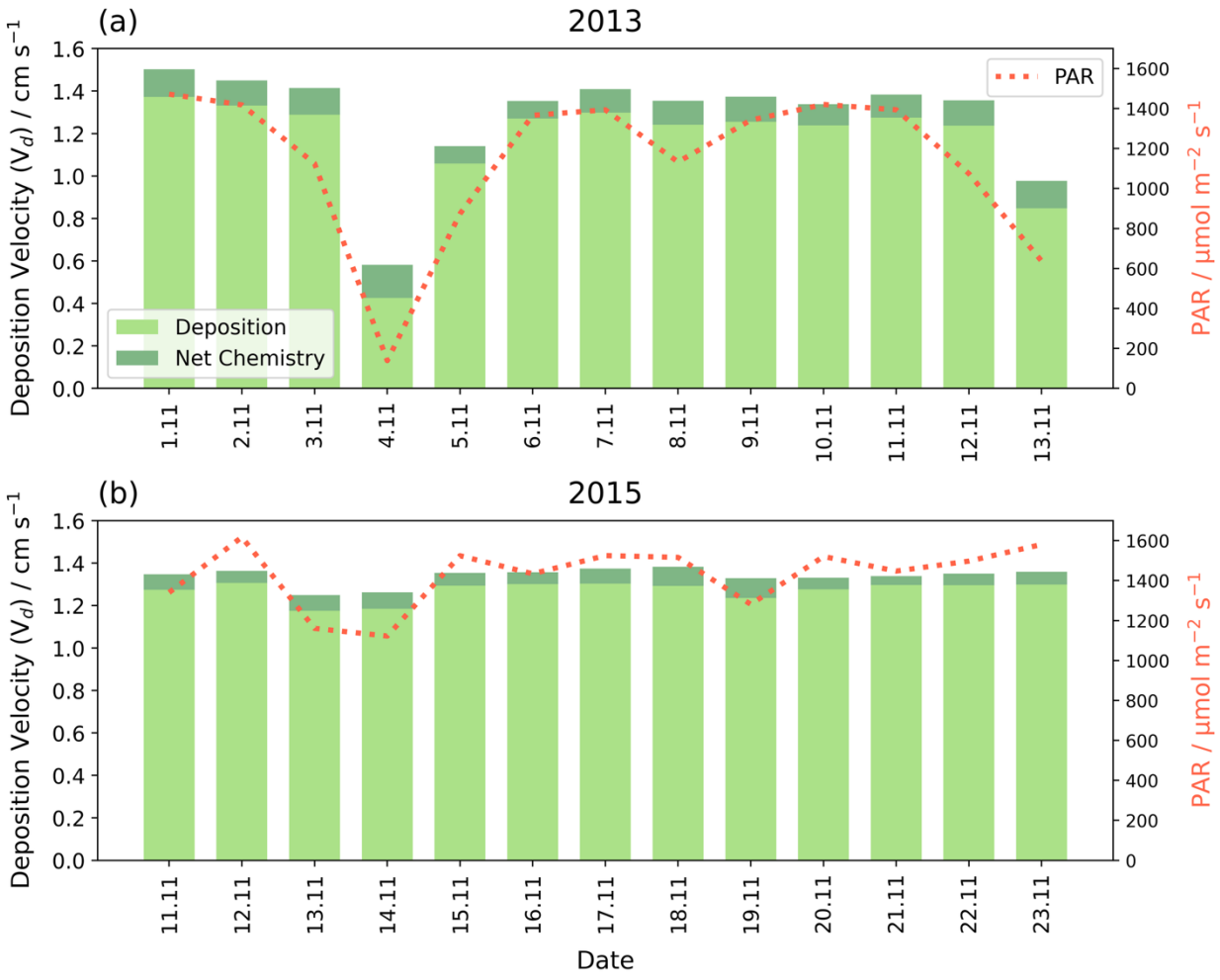

Figure S22: Daytime mean canopy-scale deposition velocity in cm s^{-1} divided into deposition (light green) and net chemistry (dark green) for (a) 2013 and (b) 2015 simulation periods. Figures also include daily mean PAR (red dotted line).

Figure S23: Daytime mean canopy-scale canopy conductance in cm s^{-1} divided into stomatal (light green) and cuticular (light green, grey stippling) conductance for (a) 2013 and (b) 2015 simulation periods.

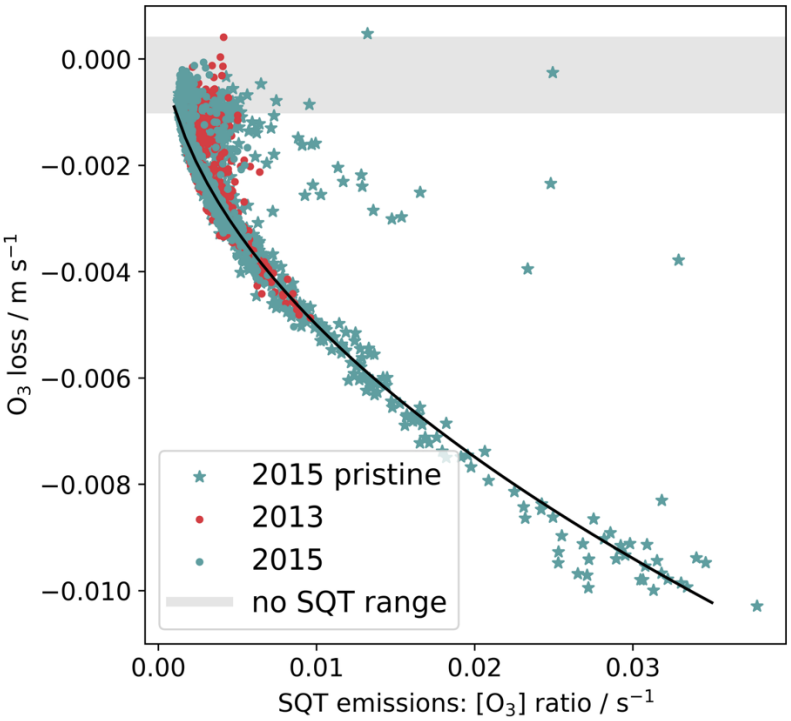

Figure S24: The relationship between the ratio of canopy sesquiterpene emissions to O_3 concentration and O_3 net chemical loss velocity to the canopy at 30 min resolution. Grey shading shows the simulated range in simulations without sesquiterpenes. The black solid line shows a line of best fit.

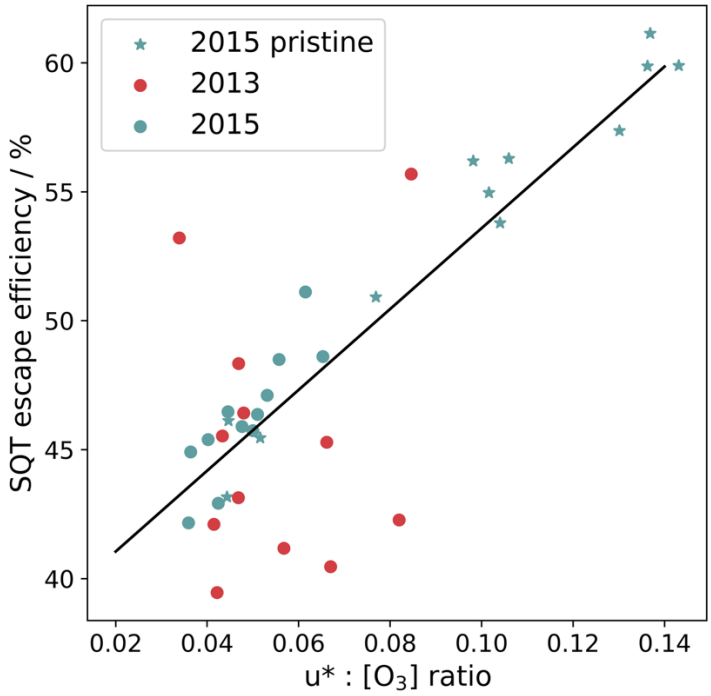

Figure S25: The relationship between the ratio of u* to O_3 concentration and the sesquiterpene escape efficiency at a daily mean resolution. The black solid line shows a line of best fit.

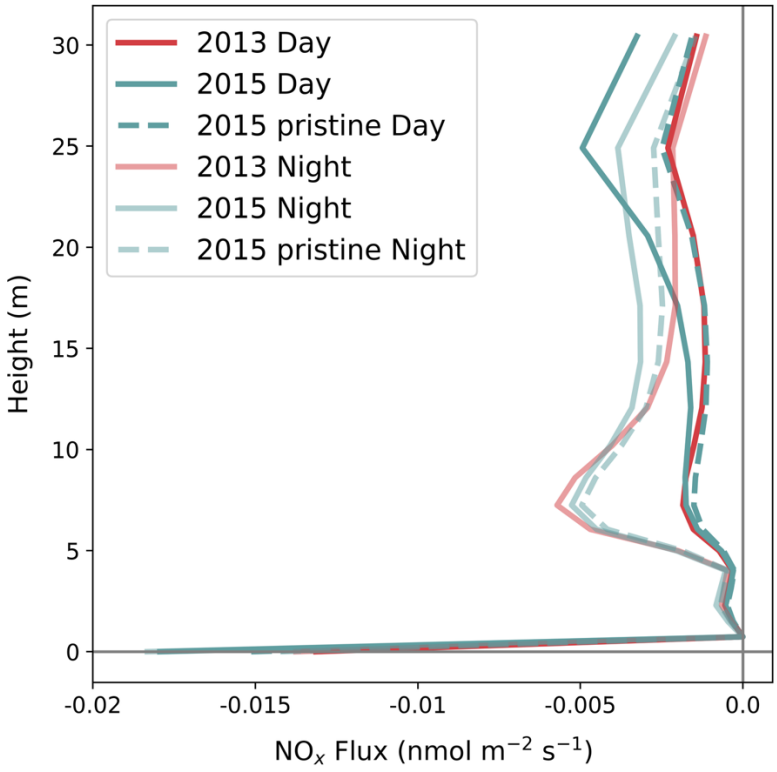

Figure S26: Vertical profiles of simulated NO_x deposition flux for simulation periods in 2013 (red lines) and 2015 (teal lines). Lighter shading indicated the nighttime mean whereas solid colours indicate daytime means.

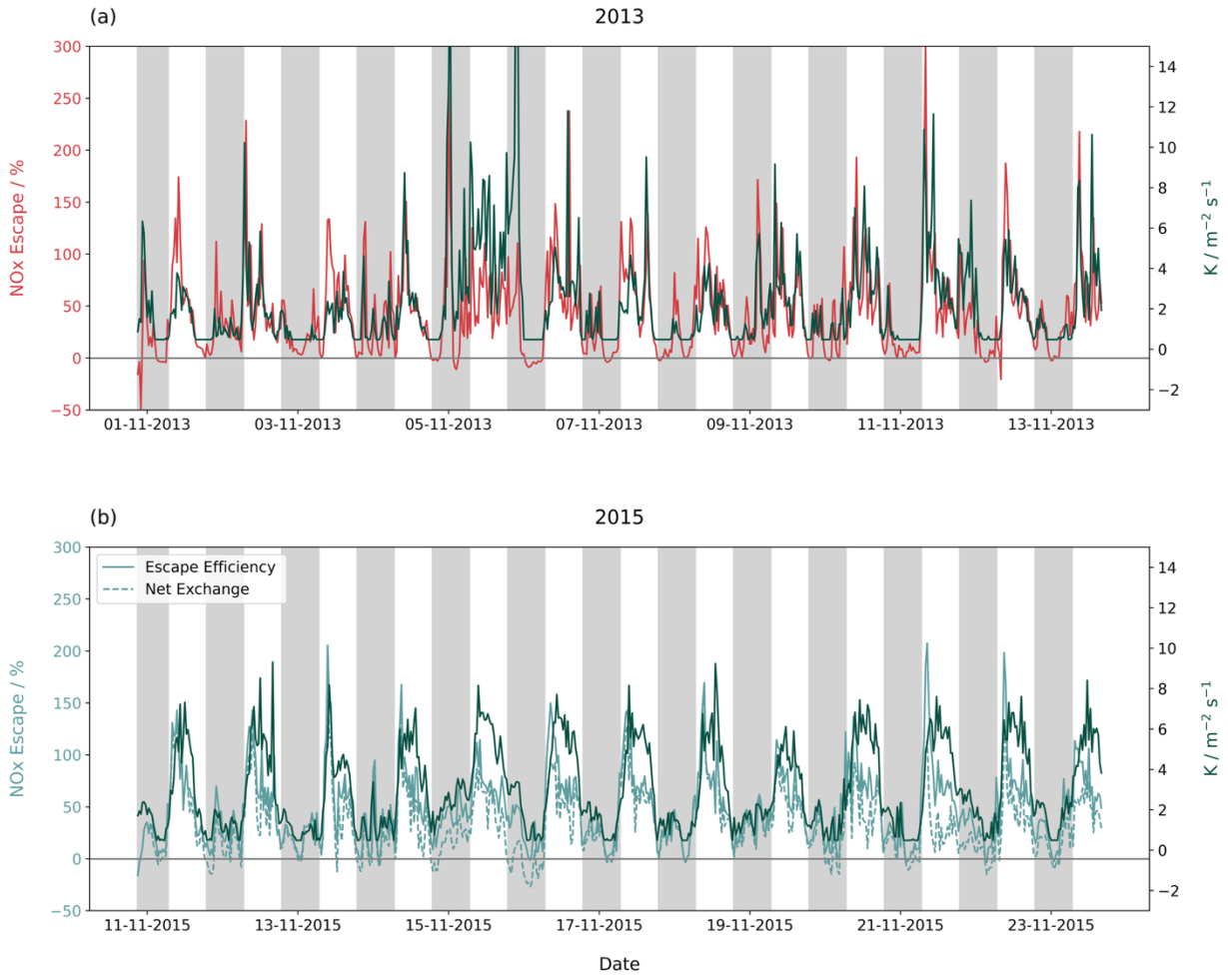

Figure S27: Time series of NO_x escape efficiency and K parameter for (a) 2013 and (b) 2015. The dashed line in (b) gives the net canopy exchange when advection is included.